Automated Tricycle as a Lunar Rescue System

Josep Rueda Collell
Researcher in Robotics.

Marc Garriga Mortensen
Software Engineer.

Rafael Espadas Pérez
Control Engineer.

Lucila Pérez Gianmarco
Researcher in Neuroscience.

I. Introduction

The lunar South Pole has become the most attractive exploration area due to the presence of water/ice [1], [2], the availability of solar energy and the geological study providing insight on its origins [3].

This region of the Moon also poses a unique set of challenges such as: extreme temperatures, variable illumination with areas permanently shadowed or illuminated [4], irregular terrain, abrasive lunar dust, low gravity, and lack of atmosphere.

The Artemis III mission will not only address these challenges, but will also mark a historic milestone by deploying two astronauts to conduct the first human exploration of the lunar South Pole. Ensuring the safety of crew members at all times is of the utmost importance; therefore, all Extravehicular Activities (EVAs) will be performed with both astronauts working closely together. Given the challenging terrain, the risk of accidents during an EVA is significant. In such scenarios, it is crucial that an astronaut can swiftly and safely rescue their crewmate, ensuring a successful return to the landing site.

NASA's current mission priorities focus on addressing Strategic Knowledge Gaps (Skgs). For instance, during the Apollo program, limited understanding of the Moon's surface led to oversized landing supports. In this proposal, we introduce our lunar rescue system designed to enhance safety for missions to the lunar South Pole.

A. Background

The surface of the Moon is covered in regolith, a smooth debris layer formed by meteoroid impacts over millions of years. Due to electrostatic forces, regolith is an adhesive dust that can agglutinate forming sharp structures that may compromise lunar exploration. Its softness varies along with its density, and the thickness and composition of its layers

differ across locations.

In addition to the regolith, the Moon's surface is scattered with rocks of various sizes, ranging from micrometric particles to boulders as large as 20 meters. This uneven and unpredictable terrain is especially pronounced in the lunar South Pole, where craters and steep elevations, including the Aitken Basin -the deepest known depression on the Moon- create further obstacles for exploration.

Additional difficulties are those related to illumination. For most regions of the Moon, a single lunar day lasts approximately 28 Earth days, with 14 days of continuous sunlight followed by 14 days of darkness. However, the poles exhibit unique lighting conditions, where some areas remain in constant sunlight, while others are engulfed in darkness [5]. Permanently illuminated regions are highly valuable due to their continuous exposure to solar energy [4], while shadowed areas are of great interest due to their potential to preserve ice reserves, offering crucial resources for future exploration.

Data collected through various methodologies and missions at the lunar poles have strongly indicated the presence of water ice or other significant forms of ice, such as hydrogen ice [6], [7], [8]. These findings were further corroborated by data from the Chandrayaan-1 mission, which confirmed the existence of water ice [1], [2]. This discovery holds immense potential, as water ice could serve as a vital resource for life support, shielding for lunar habitats, propellant for lunar transportation systems, and even as a source of electrical power.

The unique illumination conditions at the lunar poles also result in distinct temperature profiles. While most regions of the Moon experience temperatures ranging from 120 ºC to -150 ºC [9], the poles exhibit more extreme variations. In permanently illuminated areas, the average temperature is around -50 ºC. In contrast, shadowed regions such as the Hermite crater near the North Pole have recorded the lowest temperatures in the solar system, plummeting to 30 degrees below absolute zero (-30 K or -303 ºC).

B. Solution Description

The proposed solution is an automated tricycle designed to be compactly carried on the astronauts' backs during extra-vehicular activities (EVA). In the event of an emergency, an astronaut can load an incapacitated crew member onto the tricycle and activate its autonomous navigation system (Figure 1), facilitating a safe and efficient return to the landing site.

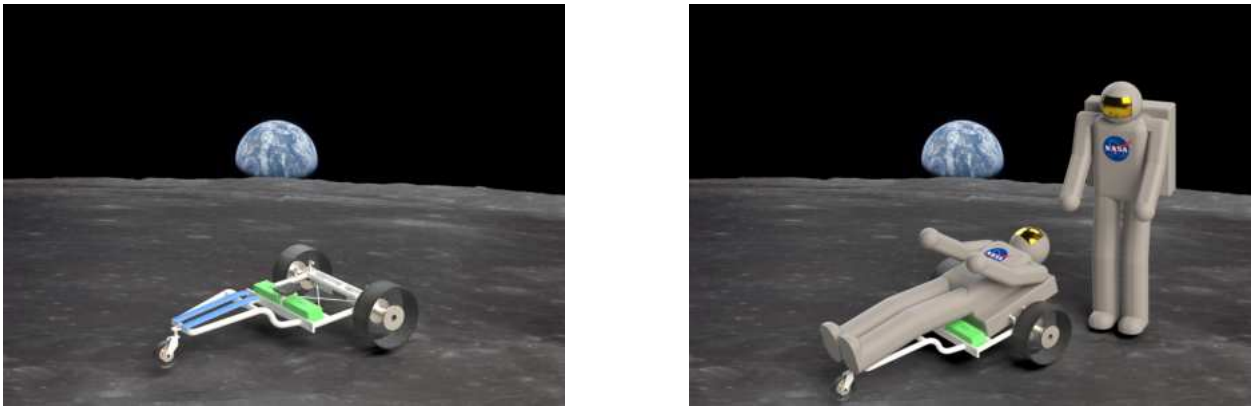

Fig. 1 Solution deployed with and without payload

The proposal aims to enhance lunar rescue missions by offering the following key features:

- **Low Mass**: Weighing no more than 23 kg for ease of transport and deployment.
- **Compact Design**: Minimal volume to ensure efficient storage and portability.
- **Rescue Range**: Capable of operating within a maximum rescue distance of 2 km.
- **Terrain Adaptability**: Designed to navigate rough lunar terrain, including slopes and craters.
- **Environmental Resilience**: Resistant to extreme temperature variations, lunar dust, and vacuum conditions.
- **Single-Astronaut Operation**: Fully operable by a single crew member during emergencies.
- **Risk Mitigation**: Ensures no additional risk to astronauts during rescue operations or EVAs.
- **Spacesuit Compatibility**: Requires no modifications to existing spacesuits.
- **Anthropometric Design**: Accommodates a large range of astronaut body sizes and shapes.
- **Mission Flexibility**: Versatile and adaptable to various mission requirements and scenarios.

This proposal will provide a comprehensive overview of the system's composition and the detailed analyses conducted to ensure its suitability for the intended mission.

II. Vehicle Composition

The tricycle consists of a frame -where the incapacitated astronaut is positioned-, three wheels, two motors, batteries, six rotating screws, and various electronic components (Table 1). The design was meticulously optimized to minimize mass while maintaining reliability in the harsh lunar environment. This section provides a detailed explanation of the tricycle's components and its overall design.

Component	Total Weight (kg)	Total Cost (M$)
(2) Wheels	4.0	2M$
Caster wheel	1.0	0.15M$
Frame	8.327	15000$
(6) Rotating screws motors	0.36	1372$
(2) Wheel motors	3.35	2095$
(2) Gearboxes	1.81	1191$
Power Supply	3.0	500$
Electronic components	0.6	10000$
Hand/Wrist band	0.1	10000$
Total	**22.547**	**2.3M$**

Table 1 List of Components, Estimated Weight and Cost

A. Frame

The frame's geometry is specifically designed to accommodate the incapacitated astronaut in a single position, optimizing their fit within the vehicle.

When designing, all calculations were based on accommodating an astronaut up to 2 meters tall and 1 meter wide, with a total mass of 343 kg. As a result, the frame can fit individuals of this size or smaller. To support this weight while maintaining a lightweight structure, we selected robust materials capable of withstanding extreme temperatures and the abrasive nature of lunar regolith.

The frame is made out Bismaleimide (BMI), a high-performance composite material known for its exceptional temperature tolerance, toughness, and lightweight properties compared to traditional metals. BMI is highly plastic in its uncured state, allowing for the fabrication of complex parts with relative ease. Widely used in the aviation and space industries [10], this material is well suited for the demanding conditions of lunar exploration. With a density of 1.25 g/cm^3, our calculations estimate the total frame mass to be as low as 8.327 kg, ensuring both strength and minimal weight.

The frame is constructed using hollow profiles, similar to those found in conventional bicycle frames. This design choice significantly reduces mass while providing internal space to route electric cables. By enclosing the cables within the frame, they remain sealed and protected from lunar dust, preventing damage to sensitive electronic components.

Additional features incorporated into the frame include:

- Six Rotating Screw Motors (MLSX8A05): These ensure proper attachment in various scenarios. Four motors are used to embed the folded vehicle to the astronaut's backpack and to secure the incapacitated crew member during rescue operations.

  The remaining two motors prevent the vehicle from folding unintentionally during use. Additionally, the frame's geometry ensures that the astronaut's weight keeps the vehicle securely unfolded, with the screw motors providing extra robustness for reliability.
- Luminescent Coating: The frame is coated with a luminescent paint that captures light from available sources, such as sunlight during the day or the light emitted from an astronaut's helmet or torch at night. This feature enhances visibility in low light conditions, making it easier to locate and load the injured astronaut without adding significant weight or volume to the solution.
- Plastic Seat and Leg Supports: A small plastic seat is included to support the lower body of the incapacitated astronaut, along with two bands to secure the legs near the caster wheel, ensuring comfort and stability during transport.
- Rubber Band: A durable yet flexible rubber band has been included to serve two main purposes. The first one is wrapping the folded tricycle to hold it in this configuration while carried on the astronaut's back. The second purpose is securing the hands of the incapacitated astronaut together, allowing the arms and hands to rest comfortably between the thighs and preventing their protrusion from the vehicle. The band is robust enough to maintain this position but can be easily removed by the incapacitated astronaut if necessary.
- Manual Lock Overrides: Because our proposal relies on screw motors which rely on batteries, there are potential scenarios in which the incapacitated crew member might be trapped on the vehicle. To prevent this from happening, the four motors that hold the vehicle and the astronaut together, would have an accessible mechanical lock overrides to detach the astronaut from the frame.

The frame is designed to be simple yet highly functional, featuring a main folding joint for easy transportation (see Section V. Collapsibility for details). Additionally, the main wheels can be disassembled from the frame during space flights, resulting into a compact solution, optimal for storage and transport conditions.

B. Wheels

The vehicle is equipped with three wheels: two front driven wheels for propulsion and a single rear caster wheel for stability and maneuverability.

1. Driven Wheels

For the driven wheels, the same wire mesh design used during the Apollo 15-17 missions is proposed. This choice offers several advantages: a) proven efficiency and reliability in the lunar environment [11], b) ease of manufacture due to existing expertise, and c) lightweight construction compared to more modern alternatives, such as the wheels designed for the VIPER rover.

The original Apollo lunar rover wheels had a mass of 5.48 kg, a diameter of 0.818 m and a width of 0.229 m [12], [13]. To reduce the torque required to propel the tricycle, the wheel diameter was decreased to 0.5 m. This modification also led to a reduction in mass, with each wheel now weighing approximately 2 kg, resulting in a total mass of 4 kg for the driven wheels.

Regarding the steering architecture, a differential steering system has been selected to transmit the motor's force to the wheels and generate movement. This choice was made over alternatives such as Ackermann steering or skid steering due to its mechanical simplicity and superior maneuverability. However, precise control is required to maintain straight trajectories, as the system relies on the speed difference between the two driven wheels to control the direction.

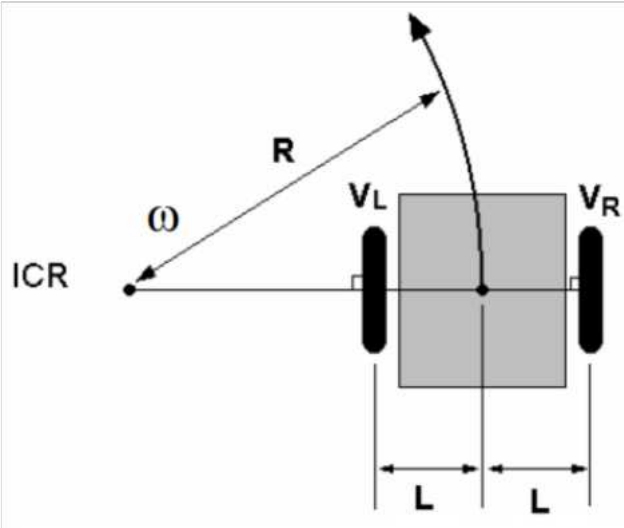

Fig. 2 Schematics of a vehicle with differential steering

The vehicle features two traction wheels positioned on an axis perpendicular to the direction of travel (Figure 2). To ensure stability and maintain horizontality, supports or caster wheels are typically employed. The wheels serve a dual purpose, functioning as both driving and steering mechanisms. By independently controlling the angular velocities of the left and right wheels (ω_l and ω_r), the vehicle achieves precise movement and navigation across complex terrain. The linear (v) and angular (ω) velocities of the vehicle are given by the following equations of motion:

$$v = r_{wheel} \cdot \frac{\omega_{\mathrm{l}} + \omega_{\mathrm{r}}}{2}$$

$$\omega = \frac{r_{wheel}}{2l} \cdot (\omega_l - \omega_r)$$

Here, w_r represents the wheel radius, and l is the distance from the center of the axis formed by the driven wheels to one of the wheels. This design ensures enhanced agility and streamlined efficiency while maintaining precise control over the vehicle's movement without the necessity to invest additional weight into another direction system.

2. Caster Wheel

The primary function of the caster wheel is to keep the tricycle stable. With an estimated diameter of 0.25 m and a mass of 1 kg, the wheel is designed to provide support while minimizing weight. To prevent drifting, the design incorporates a brake system that restricts rotation along the vertical axis when necessary (for further details, see Section III.G). The caster wheel utilizes the same proven materials as the driven wheels, reducing costs and leveraging existing know-how.

C. Motors

The vehicle is propelled by brushless direct current electric motors (BLDCs). BLDCs are three-phase synchronous motors that operate using a three-phase signal. To power these motors, a DC voltage is converted into a three-phase square wave using electronic controllers based on three-phase inverters.

BLDC motors are widely used for their high efficiency as they eliminate voltage losses associated with brushes. This brushless configuration also reduces maintenance needs and removes mechanical limitations tied to brush wear. Additional advantages include: (a) high reliability even at elevated speeds, (b) an excellent speed-to-torque ratio, enabling high-speed operation under load, (c) a compact size due to superior thermal properties, (d) improved heat dissipation, as the windings are located in the stator and connected to the motor casing, (e) a broad operational speed range, and (f) minimal electromagnetic interference (EMI) generation. However, BLDC motors require complex and costly electronic controllers for operation.

A planetary gearbox with a reduction ratio will be used to meet the tricycle's torque and RPM requirements. Although BLDC motors do not always require a gearbox, this design demands one, given the high torque needed to rescue an injured astronaut. The gearbox amplifies the motor's torque output by reducing its angular speed, ensuring the tricycle performs effectively under load.

For weight estimation, Maxon Motors components were used as a reference. Each motor has an approximate mass of 1.675 kg (model: IDX 56 L, 56 mm, brushless, with integrated electronics and brake, I/O), and each attached gearbox

weighs 0.908 kg (model: Planetary gearhead GPX 52 UP, Ø52 mm, 3-stage). The selected motor delivers 400 W of power, a nominal torque of 7790 mN·m, and a maximum drive speed of 6000 rpm, with compatibility for a 12-48 V power supply. The chosen gearbox features a 62:1 reduction ratio, three stages, and a maximum continuous torque of 45 N·m. Combined, the two motors and gearboxes contribute a total mass of 5.166 kg.

D. Power Supply

The batteries will be properly insulated to withstand the extreme lunar temperatures and recharged at the base after each rescue mission. Lithium-based secondary batteries are commonly used in spacecraft technologies, given their high energy-weight ratio [14], and are therefore the ones envisioned for this vehicle. Given its power requirements, the power supply's estimated weight is approximately 3 kg, including the charger.

An alternative, as discussed in [15], is to 3D-print batteries using lunar regolith at the Artemis base camp. Given the scarcity of lithium on the Moon, sodium-ion (Na-ion) technology emerges as a more suitable choice for in-situ resource utilization.

The power supply will be positioned beneath the astronaut's seat, optimizing the vehicle's ergonomics and ensuring easy access for recharging or replacement.

E. Other Electronic Components

In addition to the primary mechanical and propulsion systems, the tricycle incorporates several electronic components. These components include a LIDAR system, a Lunar Positioning System (lunar GPS), an Inertial Measurement Unit (IMU), a Central Processing Unit (CPU), and a remote controller. Each plays a critical role in enabling the vehicle to navigate the lunar terrain, maintain stability, and execute commands effectively.

- **LIDAR**: the Light Detection and Ranging is vital for a) detecting and avoiding obstacles on the lunar surface, b) generating detailed maps of the terrain and c) facilitating autonomous navigation, by identifying the safest and most efficient routes. Two Garmin Lite V3 units, one mounted at the front and the other at the rear, are selected for this purpose, with a combined weight of 0.044 kg.
- **Lunar Positioning System**: Similar to Earth's GPS, this enables (a) real-time tracking of the vehicle position, which is essential for navigation, and (b) route optimization alongside the LIDAR. For current state-of-the-art technologies, refer to section IV. Control, subsection B. Location.)
- **IMU**: The Inertial Measurement Unit is key for maintaining stability. It measures (a) orientation and (b) speed, providing critical data to assist during navigation. The selected model is the Honeywell HG4930, with an approximate weight of 0.180 kg.
- **CPU**: The Central Processing Unit acts as the brain of the tricycle, (a) coordinating all subsystems and (b) processing

collected data. The NVIDIA® Jetson AGX Orin™ 32GB is proposed for this role, with a weight of approximately 0.350 kg.

- **Remote controller**: A remote controller is included to send commands to the vehicle and execute specific actions. Its weight is estimated at 0.100 kg.

III. Vehicle Analysis

A. Constants and Variables

The following table (Table 2) describes the vehicle parameters and its surrounding environment:

Parameter	Symbol	Value	Description
Environment Parameters			
Moon Gravity	g_{moon}	1.625 m/s^2	Gravitational acceleration on the Moon.
Slope Angle	θ	20°	Maximum slope angle.
Rolling Coefficient	C_{rolling}	0.05	Rolling resistance coefficient.
Physical Parameters			
Astronaut Mass	$m_{\text{astronaut}}$	343 kg	Mass of the astronaut.
Vehicle Mass	m_{vehicle}	23 kg	Mass of the vehicle.
Total Mass	m_{total}	366 kg	Combined mass of astronaut and vehicle.
Wheel Radius	r_{wheel}	0.25 m	External radius of the wheel.
Wheel Internal Radius	$r_{\text{wheel,internal}}$	0.23 m	Internal radius of the wheel.
Wheel Mass	m_{wheel}	2.0 kg	Mass of a single wheel
Caster Wheel Mass	m_{caster}	1.0 kg	Mass of the caster wheel.
Caster Wheel Radius	r_{caster}	0.125 m	Radius of the caster wheel.
Caster Wheel Internal Radius	$r_{\text{caster,internal}}$	0.105 m	Internal radius of the caster wheel.

Table 2 Environment and physical parameters

B. Velocity and acceleration

- **Total Distance** (d_{total}): The total distance the vehicle expects to cover.

$$d_{\text{total}} = 2\,\text{km} = 2000\,\text{m}$$

- **Speed** (v_{speed}): The maximum speed of the vehicle in km/h.

  In [16], the measured preferred transition speed (PTS) between walking and running in actual lunar gravity was found to be $1.42 \pm 0.24\ m/s$, which translates to approximately $5.11\ km/h$ ($\approx 1.23\ m/s$). Therefore, assuming a maximum astronaut speed of $5\ km/h$ is feasible.

  The motor's angular velocity is determined by the desired linear velocity. While the vehicle is designed to operate at 5 km/h to match the astronaut's pace, the motors can be dimensioned for higher speeds to accommodate additional use cases.

$$v_{\text{linear}} = 5\,\text{km/h} = \frac{5 \times 1000}{3600}\,\text{m/s} \approx 1.389\,\text{m/s}$$

So, with a maximum speed of 5 km/h (1.389 m/s), for the tricycle and the capacitated astronaut we get:

$$\omega_{\text{wheel}} = \frac{v_{\text{linear}}}{r_{\text{wheel}}}$$

Resulting in an angular velocity ω_{wheel} of 5.592 $rads/s$.

- **Angular acceleration** The angular acceleration (α_{wheel}) of the wheel is derived from the linear acceleration (a_{linear}) using the relation:

$$\alpha_{\text{wheel}} = \frac{a_{\text{linear}}}{r_{\text{wheel}}}$$

where a_{linear} is the linear acceleration of the tricycle. If we assume 10 seconds to accelerate from 0 to 5 km/h:

$$a_{\text{linear}} = \frac{v_{\text{linear}}}{t_{\text{acc}}} \quad \text{with} \quad t_{\text{acc}} = 10\,\text{s}$$

For a linear acceleration of 0.1389 m/s, we obtain an angular acceleration of 0.0347 rad/s for the driven wheels and 0.0174 rad/s for the caster wheel.

C. Moment of Inertia

The moment of inertia for a solid wheel can be calculated using the expression for a hollow cylinder:

$$I_{\text{wheel}} = \frac{1}{2} m_{\text{wheel}} \left(r^2_{\text{wheel,internal}} + r^2_{\text{wheel}} \right)$$

For the caster wheel, the same expression is applied using its specific mass and radius. Using this approach, the calculated moments of inertia are 0.1154 kg·m^2 for the driven wheel and 0.0133 kg·m^2 for the caster wheel.

D. Torque Requirement

The total torque required by the motors can be expressed as follows:

$$T_{\text{total}} = F_{\text{total}} \cdot r_{\text{wheel}} + T_{\text{inertia}}$$

Here, F_{total} represents the total force needed to overcome the combined effects of inertia, gravitational pull, and rolling resistance, while T_{inertia} refers to the total inertial torques from rotating elements. The inertia of the wheels can be calculated as follows:

$$T_{\text{inertia}} = 2\,(I_{\text{wheel}} \cdot \alpha_{\text{wheel}}) + I_{\text{caster}} \cdot \alpha_{\text{caster}}$$

In this case, $T_{\text{inertia}} = 0.0082\,\text{N} \cdot \text{m}$.

The forces involved in the tricycle's motion are calculated as follows:

- **Inertia force** (F_{inertia}): The force required to accelerate the total mass.

$$F_{\text{inertia}} = m_{\text{total}} \cdot a_{\text{linear}}$$

- **Gravitational force on a slope** ($F_{\text{gravity, slope}}$): The gravitational force component acting along the slope.

$$F_{\text{gravity, slope}} = m_{\text{total}} \cdot g_{\text{moon}} \cdot \sin(\theta)$$

- **Rolling resistance** (F_{rolling}): The rolling resistance force between the wheels and the lunar surface.

$$F_{\text{rolling}} = m_{\text{total}} \cdot g_{\text{moon}} \cdot \cos(\theta) \cdot C_{\text{rolling}}$$

The total force can then be calculated by summing the previous forces:

$$F_{\text{total}} = F_{\text{inertia}} + F_{\text{gravity, slope}} + F_{\text{rolling}}$$

Assuming a slope of 20º, $F_{\text{inertial}} = 50.84\,\text{N}$, $F_{\text{gravity}} = 203.43\,\text{N}$ and $F_{\text{rolling}} = 27.94\,\text{N}$.

Therefore, the total force results in $F_{\text{total}} = 282.2\,\text{N}$, and consequently, the total torque required by the motors is $T_{\text{total}} = 70.5577\,\text{N} \cdot \text{m}$. This torque is provided by the sum of both motors; therefore, each motor's torque will be 35.2789 $\text{N} \cdot \text{m}$.

E. Motor power

The motor power is calculated from the torque and the angular velocity of the wheel:

$$P_{\text{motor}} = T_{\text{motor}} \cdot \omega_{\text{wheel}}$$

where T_{motor} is the torque produced by the motor.

In our case, $P_{\text{motor}} = 196\,\text{W}$.

We have selected a commercial motor that meets our torque and velocity requirements. The specifications of this motor are detailed in Section II, Vehicle Composition, Part C of this proposal. Its nominal power is 400 W, and its efficiency is 0.94, which results in an electrical consumption of 425.53 W.

F. Energy requirements and Battery capacity

The total energy required for the tricycle to cover the desired distance is computed based on the power consumption and the time required:

$$t_{\text{total}} = \frac{d_{\text{total}}}{v_{\text{linear}}}$$

The total energy required in watt-hours is:

$$E_{\text{total}} = P_{\text{total}} \cdot t_{\text{total}}$$

where P_{total} is the total power drawn by the motors and other electronic components.

In the most unfavorable scenario, where the motor operates at maximum power consumption (which is unlikely, as our power needs are less than half its nominal power), this consumption is 425.53 W. The other components are estimated to consume approximately 25 W, resulting in a total electrical power consumption of 876 W.

Since the battery efficiency is less than 100%, the energy required from the battery is increased by the inverse of the efficiency:

$$E_{\text{required}} = \frac{E_{\text{total}}}{\eta_{\text{battery}}}$$

where $\eta_{\text{battery}} = 0.8$ is the efficiency of the battery.

Finally, the required battery capacity in ampere-hours is:

$$C_{\text{battery}} = \frac{E_{\text{required}}}{V_{\text{battery}}}$$

where $V_{\text{battery}} = 48\,\text{V}$ is the battery voltage.

In our calculations, $E_{\text{total}} = 350.43\,\text{W} \cdot \text{h}$, $E_{\text{required}} = 438\,\text{W} \cdot \text{h}$, and consequently, $C_{\text{battery}} = 9.13\,\text{A} \cdot \text{h}$.

G. Stability Study

When designing the tricycle, our primary concerns were the risk of tipping over, falling, or drifting due to improper weight distribution or encountering a bump under a wheel.

To evaluate the design's suitability and enhance its stability, we recreated the tricycle model in MATLAB [17] and calculated the reaction force at each wheel, considering various ground inclinations.

The script was developed meant to be user-friendly allowing easy scalability and flexibility, allowing quick adjustments and rapid testing of new ideas (Annex 1). Multiple simulations were conducted to determine the most effective and practical design for the task, adjusting factors such as weight distribution, wheel dimensions, frame size and inclination (Figure 3). For the analysis, the astronaut's body was modeled with a 1-meter length for both the core and legs, assigned masses of 243 kg and 100 kg, respectively.

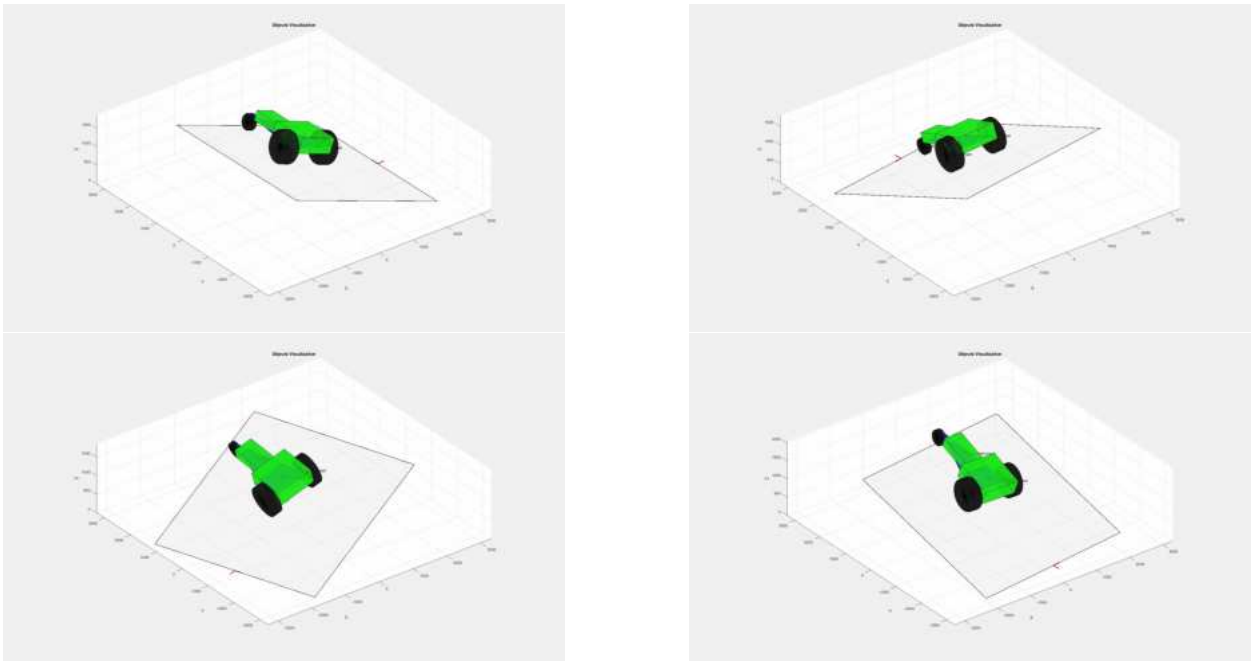

Fig. 3 Tricycle with incapacitated astronaut on multiple inclines

This study provided us with valuable insights that guided several key design decisions. For instance, it confirmed that a reclining position for the astronaut offers significantly greater stability compared to a sitting position, due to the lower center of gravity (Figure 4).

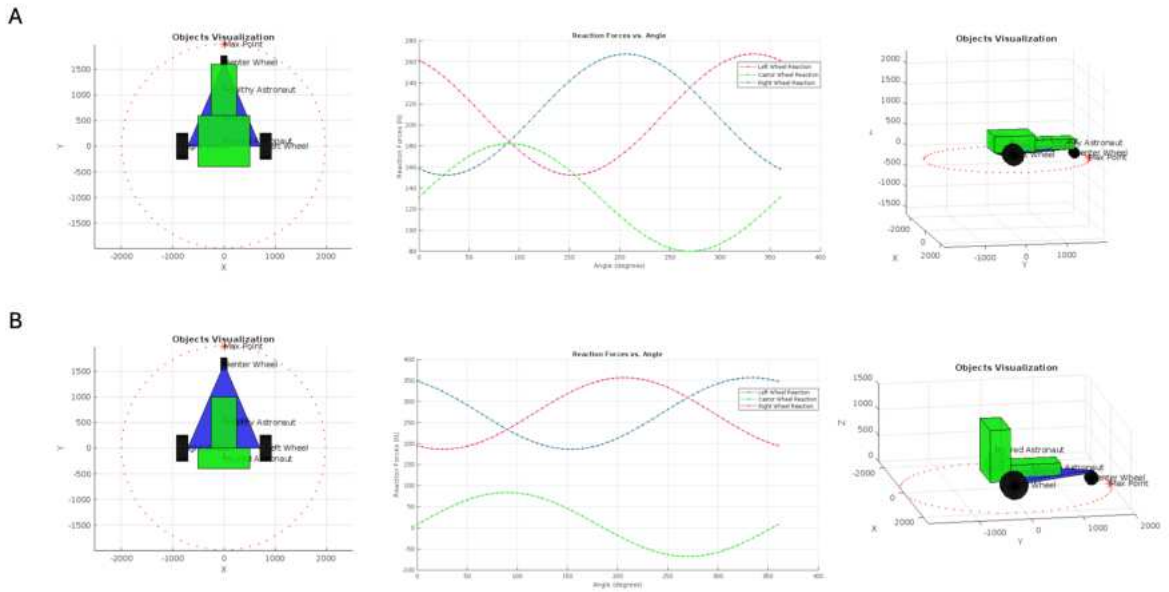

Fig. 4 A. Reaction force on wheels in reclining configuration. B. Reaction force on wheels in sitting configuration

Given that the tricycle is designed with a caster wheel, we considered the potential for drifting when diagonally climbing an incline, where the driven wheels (front) and the caster wheel (rear) may become misaligned. To prevent this drifting, a brake is installed on the vertical axis of the caster wheel blocking the rotation along the aforementioned axis, virtually transforming the caster wheel into a rigid wheel, forcing it to maintain its direction. This is particularly useful when the vehicle faces a ramp and the necessity to climb it, following a non straight path, which could cause drifting due to the natural lack of lateral friction of a caster wheel.

This stability study focused on two vital factors: preventing drifting and tilting, both of which our tricycle effectively addresses, by ensuring that all wheels keep their reaction forces within a boundary. Preventing drifting is achieved by maximizing the load on the driven wheels (instead of the caster wheel), and this is maintained across all angles (Figure 5). The second is ensuring that none of the wheels experience a reaction force of zero or less. Having imposed in the simulation, that all wheels must maintain contact with the ground, a scenario where a reaction force is below zero would indicate that a wheel has lost contact with the ground, causing the vehicle to tilt and potentially endangering the incapacitated astronaut. In our proposal, the lowest reaction force at any point is 80 N at the caster wheel (Figure 5), which is well above the threshold for tilting.

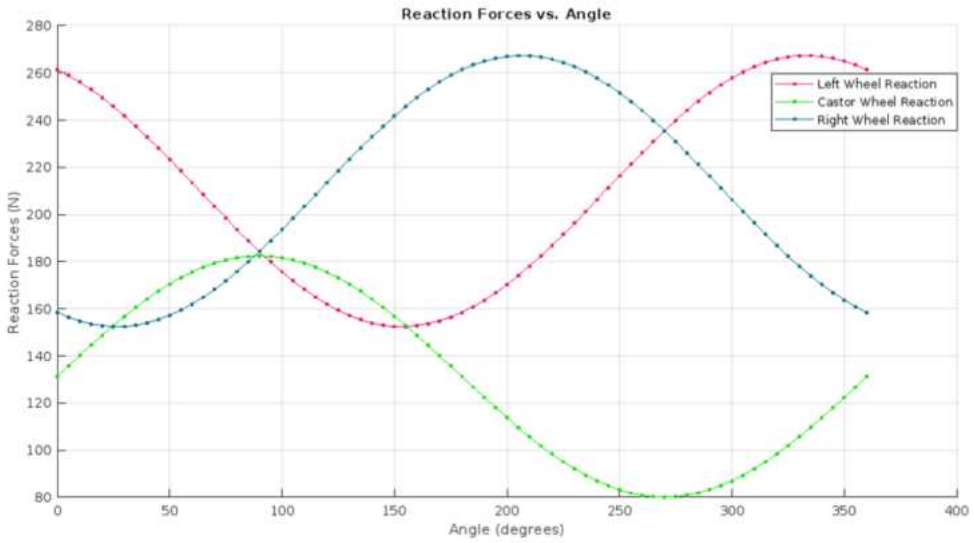

Fig. 5 Wheels reaction forces vs angle

IV. Control

Given limited mobility of astronauts, the proposal uses short-range radio communication to facilitate procedures such as unloading the vehicle and securing the crew member.

The proposal uses basic unidirectional signals, requiring the vehicle to maintain a functioning receiver throughout the entire mission. Additionally we consider the worst-case scenario where astronauts have no interface to control the available electronic devices. To address this, our proposal equips each tricycle with a remote control for operation.

A comparable example is the Remote Keyless Entry (RKE) technology, the current technology used to remotely unlock a car using a small radio emitter, typically embedded within the car key. According to an application note by NXP Semiconductors, the power consumption of an RKE module can drop to approximately 100 μA in low-power mode (as seen in older commercial models like ATA5795C [18] or MPC5516 [19]).In our case, using this same technology, we will be able to issue the following set of actions. We consider the power consumption in sleep or idle mode to be so small that it can be neglected.

The actions that can be triggered are as follows:

- **Detach pilot**: A command that retracts the four rotating screw motors from the Primary Life Support System (PLSS). This function is used to unload the vehicle from the astronaut's back and also to detach the injured astronaut from the vehicle upon arrival.
- **Attach pilot**: A command that advances the four rotating screw motors to secure the vehicle to the PLSS. This function

is used to fasten a crew member to the unfolded tricycle or to reattach the folded tricycle back to the astronaut's PLSS.

- **Lock vehicle**: A command that retracts two rotating screw motors, allowing the vehicle to be folded.
- **Unlock vehicle**: A command that advances two rotating screw motors to secure the unfolded tricycle, preventing it from folding.
- **Turn On**: A command that powers the wheels' motors, keeping the vehicle stationary and preventing movement, useful to further facilitate the task of loading an injured astronaut into the vehicle.
- **Turn Off**: A command that cuts power to the wheels, stopping their movement.
- **Go to**: A command that begins the journey to the destination, enabling movement on the wheels, and locks them upon arrival.
- **Stop**: A command that halts current movement and locks the wheels in place.

For a detailed overview of the steps required for deployment, refer to Section VII: Deploy.

A. Location

Lunar Orbiter Laser Altimeter (LOLA) is responsible for 3D mapping the lunar surface's global topography at high resolution. Thanks to the data collected by LOLA in recent years [20], we now have detailed, high-resolution maps of the Moon, including its south pole.

Regarding lunar localization, there are promising prospects, including:

- A reverse-ephemeris approach, where small satellites orbiting the Moon serve as fixed reference points with a known ephemeris. The satellite trajectories, tracked from Earth's perspective, are discussed in [21].
- A more recent collaboration between the Italian Space Agency (ASI) and NASA, aiming to assess whether GNSS signals can be used for precise positioning and timing on the Moon's surface [22]. Scheduled for launch on January 15, 2025, this initiative could serve as a key step toward developing a lunar GPS system for long-term exploration.

The tricycle is designed to capture its current location upon boot-up, using its lunar GPS as well as its LiDAR sensors.

B. Movement control

Once deployed the tricycle will continuously reevaluate its route in real-time. If it encounters unrecorded obstacles or changes in the terrain, it will assess whether it remains on course or if adjustments to its current location are necessary.

These components are outside the scope of this proposal. The vehicle is designed to require no direct intervention from the incapacitated astronaut. Instead, it is the capacitated astronaut who interacts with the tricycle interface.

The tracking, as well as the control itself, will be carried out with an onboard flight software based on the NASA

cFE/cFS middleware, [23], reusing as much as possible from the VIPER rover. The capacitated astronaut will be in charge of supervising that the evacuation is done both successfully and safely at all times, as she/he will also be returning to the base at the same pace as the tricycle. If needed and in unexpected conditions, the tricycle could be pulled.

V. Collapsibility

One key aspect of this solution is its collapsibility. The main focus is the tricycle's reliability to complete the rescue mission, while keeping in mind that it should be as light/compact as possible. In order to fulfill both goals, a single hinge was used in the design, minimizing the weak points, while enhancing transportation efficiency, both as payload when sending it EtM (Earth to Moon), and during EVAs.

The tricycle is designed with a single center foldable joint, pleating the device outwardly. This ensures a reliable and prompt deployment without the need to adjust wheel alignment or moving parts, although at the expense of more volume.

Fig. 6 Folded/Unfolded tricycle

VI. Transport

A. Earth to Moon

For Earth to Moon (EtM) transport the tricycle could be disassembled into smaller parts (wheels, the frame split into two pieces) allowing for better space optimization, the assembly process would then be carried out in the lunar base without spacesuits. If we lack the infrastructure to assemble the tricycle on the Moon, it shall be folded for transport as a single unit.

B. Lunar missions

On the Moon, tricycles would be securely attached to the astronauts Primary Life Support System (PLSS; Figure 6) using four screw motors to lock the vehicle in place. Additional details will be provided in the following section.

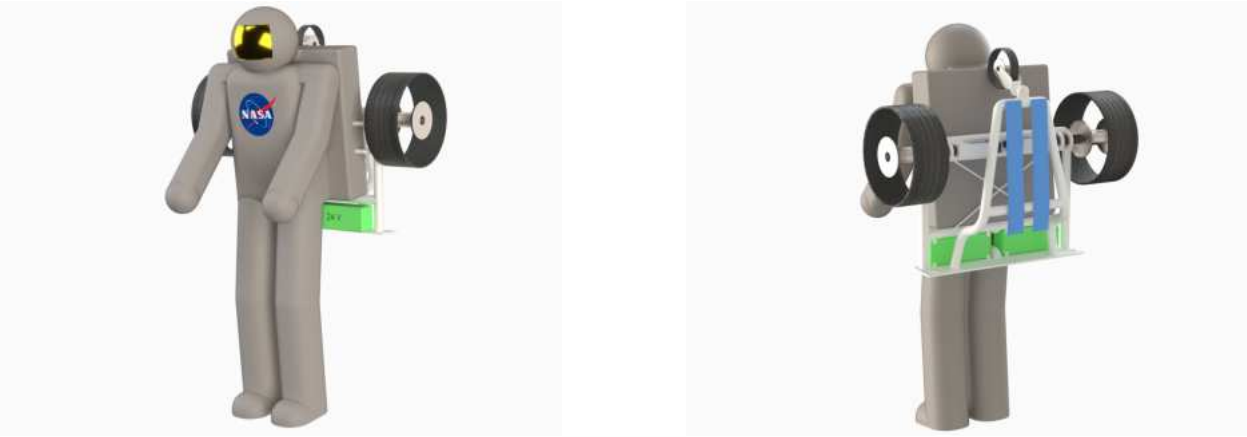

Fig. 7 Astronaut with folded tricycle on PLSS

VII. Deploy

When on a rescue mission, the tricycle must be deployable by a capacitated astronaut wearing a spacesuit. Therefore, its assembly must be easy, fast and reliable. The necessary steps to assemble, load, unload and disassemble the tricycle will be outlined in this section.

On the following steps the worst case scenario is assumed, where the vehicle is mounted on the capacitated astronaut and he/she is walking to rescue the incapacitated crew member.

A. Transport unload

1) Using a radio signal from the remote control, the turn on command is sent, locking the wheels.
2) Detachment of the tricycle from the PLSS. Using a radio signal from the remote control, the vehicle is freed from the PLSS by electrically retracting the four rotating screw motors.
3) Once the detach signal is triggered, the vehicle falls straight to the ground as expected.

B. Assemble

Once the vehicle has touched ground, preparations are required for its assembly.

1) Remove the rubber band that holds the frame safely folded.
2) Apply force to unfold the tricycle.
3) Trigger the "lock vehicle" command using a radio signal that advances two rotating screw motors, preventing the

frame from folding back when carrying the astronaut.

C. Load up

1) The capacitated astronaut carries and places the incapacitated crew member on the vehicle, fitting the PLSS to the designated zone between the driven wheels (Figure 7).
2) The capacitated astronaut triggers the "attach" command so that the incapacitated crew member is securely attached to the vehicle, making use of the same four rotating screws that keep the folded tricycle secured to the astronaut's PLSS.
3) The capacitated astronaut uses the rubber band (which was previously securing the frame folded) to bound the wrists of the incapacitated crew member. Then, he/she places the hands resting between the legs, to prevent them from falling of the vehicle during the rescue mission.
4) The capacitated astronaut activates the "go to base" command, and they initiate the route back to base.

D. Direct Assemble with Load up

In some situations (type of injury, sufficient space, slope of the terrain, duplicity of equipment), it might be possible and beneficial to directly assemble the tricycle on the incapacitated astronaut. The procedure presented here is the worst case scenario, rescuing a crew member without a vehicle on their back. If the astronauts found themselves in a more favorable scenario, they could skip some of the steps presented above.

Fig. 8 Incapacitated astronaut attached to the vehicle

E. Unload

1) The capacitated astronaut activates the "detach" command to release the PLSS from the tricycle, retracting the four rotating screw motors that held the astronaut in place.

2) The capacitated astronaut carries the incapacitated one out of the vehicle and follows the next step on safety protocols.
3) The capacitated astronaut issues the "turn off" command.

F. Disassemble

Once a rescue has occurred, the astronaut needs to manually fold the vehicle so that it can be repositioned in a suit for another EVA. Damage inspection and repairs are out of the scope of this theoretical proposal, but would be required in this step.

1) Manually move the vehicle to the designated area.
2) Trigger the remote "unlock" command to fold the vehicle.
3) Remove and charge the batteries.
4) While holding tight on the upper half of the frame with one hand, apply force with the free hand on the lower half, bringing the caster wheel closer to the driven wheels and folding the tricycle outwards.
5) Wrap the rubber band around the folded vehicle, to ensure that it stays in this configuration.
6) Replace batteries before going on another mission and reattach the vehicle to the PLSS.

VIII. Adaptability

This vehicle is specifically designed to overcome slopes and address any level of injury to the incapacitated astronaut, since it is independent of his/her guidance. In an ideal scenario, it will also be mostly independent of the crew-member. This section provides a list of different applications in which the tricycle could be involved, with minimal or no changes required.

If necessary, such as in the event of a motor failure, the vehicle can be pulled by an assisting astronaut while still carrying the crew member.

To facilitate this, as mentioned earlier, a planetary gearbox is used for the motors. Planetary gearboxes have two inputs and one output. One of these inputs is typically locked, causing the gearbox to function as a reducer. If needed, unlocking this input would allow the gearbox to spin freely, disabling its reduction capabilities and allowing the astronaut to pull the vehicle without resistance. However, this would require a mechanical toggle to switch between the two operating states.

Although the tricycle has been designed for human transport, it could also perform different tasks, some of which are listed here:

A. Move on demand

This vehicle can be used in any EVA. If the astronauts are capacitated, they can deploy it to move themselves, allowing a safer, faster alternative to walking to a location. Thus, this tricycle provides flexibility on lunar expeditions thanks to its ability to move autonomously on demand.

B. Cargo transport

It can carry large objects or delicate equipment over a 2 km distance, allowing better maneuverability for payload such as tools, samples, consumables or replacements, and leaving the astronaut's hands free. More adjustments can be made if sample collection is needed, such as controlling temperature of the cargo or adding shock protection.

C. Moon mapping/imaging

The tricycle is already equipped with everything needed to perform topographical mapping and imaging of areas of interest, thereby enhancing future lunar missions and providing valuable scientific data.

D. Power Source

Using the batteries as an auxiliary power source to charge devices or supply energy to other systems in case of emergency.

E. Tricycle lab

Integrating instruments for in-situ analysis, such as spectrometers/seismometers or radiation sensors, allowing the tricycle to act as a mobile lab, providing live readings during EVAs.

IX. Other Considerations

Known strengths:

- Safe and comfortable rescue transport.
- Uses simple or pre-existing components and technologies, facilitating manufacturing and maintenance.
- User-friendly design with efficient assembly and disassembly processes.
- Lightweight and easy to transport attached to the suit.
- Potential scalability and versatility, allowing adaptation to different applications
- Minimized risk using an automated solution.
- Flexibility in overcoming greater slopes or speed up when needed.
- Low wear and tear, only decreases lifetime when rescue missions are executed.
- Can be used under low-light conditions.
- Can be deployed on irregular terrain.

Known limitations:

- Structural weaknesses could appear in parts under high mechanical stress, as a direct consequence of volume reduction.
- Energy efficiency may be compromised when carrying heavy loads beyond the specified limits or when navigating very uneven terrain.
- The solution relies partially on localization infrastructure that is still being established.
- For efficient operation, the system must carry a payload. Low weight might negatively affect performance.
- Upon navigation failure human intervention is required.

A. Improvement Possibilities

Given the mass limitations for this challenge, we present here the most simplified concept that we believe can safely succeed in a rescue mission. However, if we had the luxury of increasing the mass, we would make some improvements to the design, especially on the wheels or the frame.

The wheels were one of the most challenging parts to decide on, because there are new innovative and promising designs, but they would not fit with our solution (or their specifications were not publicly available). In the case of the VIPER wheels, they were too heavy for the vehicle; while in the case of the Venturi Space wheels we could not obtain the details of dimensions and mass to use in our proposal. However, the Apollo 15-17 wheels have been used in the moon previously, which makes them a reliable solution. Moreover, NASA does have access to the cutting edge technologies in the fields and can therefore, make the improvements they deem necessary.

As for the frame, we would have liked to reinforce the BMI with carbon fiber, resulting in a composite with better mechanical properties for the task. However, the weight was critical for other parts of the vehicle, so we could not include this material.

To overcome the possible failure of location systems, a new rescue command "follow" could be added, which would make the vehicle safely follow the capacitated astronaut at a distance in order to return to base, thus delegating the navigation system to the astronaut instead.

B. Costs

Regarding the wheels, considering the proposed design is based on the Apollo missions 15-17 wheels, which have already been developed and used on the moon, would imply a reduction of the costs associated with research, prototyping, and testing. As a reference, VIPER's development cost was $609.6 million [24], and it is estimated that 5% to 15% of VIPER's total development cost was assigned to the wheels (approximately $60 million, $15 million per wheel).

In 1971, the total cost of the Apollo Lunar Roving Vehicle was $38 million, which would nowadays translate to $290 million. Following the same estimation as the one done for the VIPER, this would mean that the Apollo wheel development was approximately $30 million. Since these have already been designed and tested in the past, we calculate that the cost of manufacturing the smaller Apollo wheels suggested in this proposal, would be approximately of $1 million per wheel.

For the frame, and assuming that raw BMI resin typically ranges from $30 to $100 per kg, for 8 kg, the cost could range from $240 to $800. Adding the manufacturing and processing costs, a high-end estimate of $15.000 is expected. Concerning the motors, and as mentioned before, Maxon motors have been used as reference, the estimated price is $3.500, taking gearboxes and necessary electronics into account. As for power supply, commercial models have been considered for weight and cost estimation, but an ad-hoc solution would be more suitable for the project, roughly approximating 2.5 kg and $500. Finally, for sensors, actuators, CPU and small electronic components, an additional 0.6 kg and $10.000 are estimated. The overall approximate cost for the proposal would be at 2.3 M$ (Table 1).

C. Reusability

If at some point the rescue system can no longer be used as such, its different parts could be reused for other purposes, such as: a) batteries could be used as storage for solar energy or to power other devices, b) the electric motors could act as generators if attached to a rotary system, c) structural elements could be employed to create tools, supports for sensors and instruments or containers, among others; d) the whole system could be re-imagined as a rover trailer or as a wheelbarrow to carry samples. All parts used in this design could easily be reused as something else, minimizing waste and adding flexibility to the missions.

X. Conclusion

It is safe to say that designing a lunar rescue system under 23 kg of mass has proven a challenging feat. In fact, some of our most innovative ideas had to be given up to fit this criterion. However, this difficulty pushed us to achieve a simple, yet promising, design.

Throughout the design process, safety was the highest priority, whether it was during the transport, rescue, or deployment stages, including the ease of use.

The simplicity of our tricycle is one of its best characteristics, making it ideal for fast extractions and potentially becoming the standard aiding solution during lunar missions. Its compact design simplifies transport during EVAs and EtM, further enhancing its functionality and ease of use in lunar operations.

We are confident that the proposal will be a great asset, aiding in pushing lunar exploration forward during the future Artemis missions.

References

[1] Li, S., and Milliken, R. E., "Water on the surface of the Moon as seen by the Moon Mineralogy Mapper: Distribution, abundance, and origins," *Science Advances*, Vol. 3, No. 9, 2017. https://doi.org/10.1126/sciadv.1701471, URL https://www.science.org/doi/10.1126/sciadv.1701471.

[2] Li, S., Lucey, P. G., Milliken, R. E., Hayne, P. O., Fisher, E., Williams, J. P., Hurley, D. M., and Elphic, R. C., "Direct evidence of surface exposed water ice in the lunar polar regions," *Proceedings of the National Academy of Sciences of the United States of America*, Vol. 115, No. 36, 2018, pp. 8907–8912. https://doi.org/10.1073/pnas.1802345115.

[3] Moriarty, D. P., Watkins, R. N., Valencia, S. N., Kendall, J. D., Evans, A. J., Dygert, N., and Petro, N. E., "Evidence for a Stratified Upper Mantle Preserved Within the South Pole-Aitken Basin," *Journal of Geophysical Research: Planets*, Vol. 126, No. 1, 2021, pp. 1–27. https://doi.org/10.1029/2020JE006589.

[4] Bussey, D. B. J., Fristad, K. E., Schenk, P. M., Robinson, M. S., and Spudis, P. D., "Constant illumination at the lunar north pole," *Nature 2005 434:7035*, Vol. 434, No. 7035, 2005, pp. 842–842. https://doi.org/10.1038/434842a, URL https://www.nature.com/articles/434842a.

[5] Bussey, D. B. J., Spudis, P. D., and Robinson, M. S., "Illumination conditions at the lunar south pole," *Geophysical Research Letters*, Vol. 26, No. 9, 1999, pp. 1187–1190. https://doi.org/10.1029/1999GL900213.

[6] Arnold, J. R., "Ice in the lunar polar regions," *Journal of Geophysical Research: Solid Earth*, Vol. 84, No. B10, 1979, pp. 5659–5668. https://doi.org/10.1029/JB084IB10P05659, URL https://onlinelibrary.wiley.com/doi/full/10.1029/JB084iB10p05659https://onlinelibrary.wiley.com/doi/abs/10.1029/JB084iB10p05659https://agupubs.onlinelibrary.wiley.com/doi/10.1029/JB084iB10p05659.

[7] Feldman, W. C., Maurice, S., Binder, A. B., Barraclough, B. L., Elphic, R. C., and Lawrence, D. J., "Fluxes of Fast and Epithermal Neutrons from Lunar Prospector: Evidence for Water Ice at the Lunar Poles," *Science*, Vol. 281, No. 5382, 1998, pp. 1496–1500. https://doi.org/10.1126/SCIENCE.281.5382.1496, URL https://www.science.org/doi/10.1126/science.281.5382.1496.

[8] Colaprete, A., Schultz, P., Heldmann, J., Wooden, D., Shirley, M., Ennico, K., Hermalyn, B., Marshall, W., Ricco, A., Elphic, R. C., Goldstein, D., Summy, D., Bart, G. D., Asphaug, E., Korycansky, D., Landis, D., and Sollitt, L., "Detection of water in the LCROSS ejecta plume," *Science*, Vol. 330, No. 6003, 2010, pp. 463–468. https://doi.org/10.1126/SCIENCE.1186986/SUPPL_FILE/COLAPRETE_SOM.PDF, URL https://www.science.org/doi/10.1126/science.1186986.

[9] Paige, D. A., Siegler, M. A., Zhang, J. A., Hayne, P. O., Foote, E. J., Bennett, K. A., Vasavada, A. R., Greenhagen, B. T., Schofield, J. T., McCleese, D. J., Foote, M. C., DeJong, E., Bills, B. G., Hartford, W., Murray, B. C., Allen, C. C., Snook, K., Soderblom, L. A., Calcutt, S., Taylor, F. W., Bowles, N. E., Bandfield, J. L., Elphic, R., Ghent, R., Glotch, T. D., Wyatt, M. B., and Lucey, P. G., "Diviner lunar radiometer observations of cold traps in the moon's south polar region," *Science*, Vol. 330, No. 6003, 2010, pp. 479–482. https://doi.org/10.1126/SCIENCE.1187726/SUPPL_FILE/PAIGE.SOM.PDF, URL https://www.science.org/doi/10.1126/science.1187726.

[10] Park, S. J., and Seo, M. K., "Element and Processing," *Interface Science and Technology*, Vol. 18, 2011, pp. 431–499. https://doi.org/10.1016/B978-0-12-375049-5.00006-2.

[11] Asnani, V., Delap, D., and Creager, C., "The development of wheels for the Lunar Roving Vehicle," *Journal of Terramechanics*, Vol. 46, No. 3, 2009, pp. 89–103. https://doi.org/10.1016/j.jterra.2009.02.005, URL http://dx.doi.org/10.1016/j.jterra.2009.02.005.

[12] GM, "LRV mobility subsystem, critical design review presentation," Tech. rep., 1970.

[13] GM, "LRV wheel assembly, technical drawings (7552941, 7553028, 7553529, 7553521, 7552939, 7552938, 7552940, 7553027, 7553199)," Tech. rep., 1971.

[14] NASA, "2022 State of the Art Small Spacecraft Technology Report," Tech. rep., Ames Research Center,, Moffett Field, California, jan 2022. URL https://www.nasa.gov/wp-content/uploads/2023/05/2022-soa-full.pdf.

[15] Maurel, A., Martinez, A. C., Dornbusch, D. A., Huddleston, W. H., Seol, M.-L., Henry, C. R., Jones, J. M., Yelamanchi, B., Bakhtar Chavari, S., Edmunson, J. E., Sreenivasan, S. T., Cortes, P., MacDonald, E., and Sherrard, C. G., "What Would Battery Manufacturing Look Like on the Moon and Mars?" *ACS Energy Letters*, Vol. 8, No. 2, 2023, pp. 1042–1049. https://doi.org/10.1021/acsenergylett.2c02743.

[16] De Witt, J. K., Edwards, W. B., Scott-Pandorf, M. M., Norcross, J. R., and Gernhardt, M. L., "The preferred walk to run transition speed in actual lunar gravity," *Journal of Experimental Biology*, Vol. 217, No. 18, 2014, pp. 3200–3203. https://doi.org/10.1242/jeb.105684.

[17] Mathworks, "Matlab," , 2024. URL https://www.mathworks.com.

[18] Atmel Corporation, "ATA5795C [DATASHEET] Ultra-low-power AVR Microcontroller," Tech. rep., nov 2014. URL https://ww1.microchip.com/downloads/en/DeviceDoc/Atmel-9182-Car-Access-ATA5795C_Datasheet.pdf.

[19] NXP Semiconductors, "MC33696 Overview," Tech. rep., NXP, sep 2008. URL https://www.nxp.com/docs/en/supporting-information/REMOTE_KEYLESS.pdf.

[20] Smith, D. E., Zuber, M. T., Neumann, G. A., Mazarico, E., Lemoine, F. G., Head, J. W., Lucey, P. G., Aharonson, O., Robinson, M. S., Sun, X., Torrence, M. H., Barker, M. K., Oberst, J., Duxbury, T. C., Mao, D., Barnouin, O. S., Jha, K., Rowlands, D. D., Goossens, S., Baker, D., Bauer, S., Gläser, P., Lemelin, M., Rosenburg, M., Sori, M. M., Whitten, J., and Mcclanahan, T., "Summary of the results from the lunar orbiter laser altimeter after seven years in lunar orbit," *Icarus*, Vol. 283, 2017, pp. 70–91. https://doi.org/10.1016/j.icarus.2016.06.006.

[21] Langley Research Center, V., Hampton, "Lunar Surface Navigation System," *Tech Briefs Magazine (Vol. 47 No. 3)*, 2023, p. 37.

[22] Powers, K., "NASA and Italian Space Agency Test Future Lunar Navigation Technology - NASA," , jan 2025.

[23] NASA's Goddard Space Flight Center, "core Flight System (cFS)," , jun 2017. URL https://github.com/nasa/cFS.

[24] David W. Brown, "NASA Canceled VIPER—That's a Good Thing," , 2024. URL https://www.supercluster.com/editorial/nasa-canceled-viper-thats-a-good-thing.